Turkish Journal of Electrical Engineering and Computer Sciences

Volume 31 | Number 2 Article 11

3-1-2023

Study of Helical Antenna Endowing Short Wire Length and Compact Structure for High-Frequency Operations and Its Exclusive Manufacturing Process

MELİH ASLAN

KAAN ŞIK

İZZET GÜZELKARA

İBRAHİM TUNA ÖZDÜR

VELİ TAYFUN KILIÇ

Turkish Journal of Electrical Engineering & Computer Sciences

http://journals.tubitak.gov.tr/elektrik/

Research Article

Turk J Elec Eng & Comp Sci
(2023) 31: 396 – 411

doi:10.55730/1300-0632.3991

Study of helical antenna endowing short wire length and compact structure for high-frequency operations and its exclusive manufacturing process

Melih ASLAN[1,*], Kaan ŞIK[1], İzzet GÜZELKARA[1], İbrahim Tuna ÖZDÜR[2], Veli Tayfun KILIÇ[1]

[1]Department of Electrical and Electronics Engineering, Faculty of Engineering, Abdullah Gül University, Kayseri, Turkey

[2]Department of Electrical and Electronics Engineering, Faculty of Engineering, TOBB University of Economics and Technology, Ankara, Turkey

Received: 26.09.2022 • **Accepted/Published Online:** 03.02.2023 • **Final Version:** 23.03.2023

Abstract: In this paper a study of a helical antenna resonating at high-frequency (HF) band with a very compact structure is reported. The designed antenna's S11 parameter magnitude change with frequency was calculated for different geometrical parameters. For each case, first, only a single parameter was changed. Then for a fair comparison, multiple parameters were changed simultaneously while the total wire length was set to be constant. Also, shifts in resonance frequencies and variations in –10 dB bandwidths were investigated. Our results show that resonance behaviour changes distinctively with the geometrical parameters and it allows shortening of the antenna wire length. For the designed antenna, the resonances shift to lower frequencies and –10 dB bandwidths around the resonances decrease as the winding wire thickness, number of turns, and turn radius increase. Whereas as the turn spacing increases the resonances shift to higher frequencies and –10 dB bandwidths widen, although the total wire length of the antenna increases. To verify the simulation results, the designed antenna was fabricated with an exclusive manufacturing process and characterized. The measurement results are in good agreement with the simulation results. It demonstrates the feasibility of the proposed manufacturing technique, which is new in the literature and enables accurate and rigid antenna fabrication with simple and low-cost steps.

Key words: Antenna manufacturing, helical antenna, HF antennas, parametric studies

1. Introduction

High-frequency (HF) band is generally used for long-distance air-to-ground or ground-to-air communications and military applications because of the low atmospheric attenuation properties in the wavelength range spanning from 10 m to 100 m in free space corresponding to HF band of 3–30 MHz [1–3]. For applications such as multimedia transmission, voice and data communication in the HF band, channel bandwidth requirements are usually around 10 KHz to 20 KHz, while for other applications in the HF band such as spread spectrum communications bandwidths greater than 100 KHz are required [4–6]. Although long wavelengths are preferred in far distance communications, as operation wavelength increases the antenna sizes also get bigger. Therefore, in addition to the performance constraints of the antenna, the size of an antenna operating in HF frequency band might also be an important restriction while designing an HF system. There are several types of antennas that are currently being used for typical HF systems such as Yagi-Uda [7], monopole antennas [8], dipole antennas [9],

*Correspondence: elektrik@tubitak.gov.tr

and bent wire antennas [10]. However, these antennas are relatively large and heavy, thus mounting standards need to be met for safe operation. Also, the packaging and manufacturing of these antennas to make them rigid enough are usually costly. Helical-shaped antennas are another type of antenna used for HF applications [11–13]. Due to their three-dimensional (3D) structure, helical antennas are lighter and smaller with respect to other HF antennas. Helical antennas are formed by winding a conductor in a helical geometry and they are typically mounted on a ground plane, which shortens the antenna length and creates a fulcrum for the antenna [14].

Helical antennas have been investigated both theoretically and experimentally in the literature [15–19]. In theoretical analysis, helical antennas are usually considered as an array of ring-shaped antennas stacked on top of each other at a certain distance [19]. However, this assumption is true only if the spacing between each turn in a helical antenna is zero. In other words, the accuracy of this assumption increases as the distance between turns in a helical antenna approaches zero. On the other hand, in a helical antenna with a low ratio of turn radius over height and a small turn number this assumption does not hold. Therefore, the precise design of a helical antenna with certain requirements is only achieved with simulations and experiments [11, 13]. Owing to the 3D architecture, there are many geometrical parameters that define a helical antenna. These parameters include the number of turns, wire length, the height of the antenna, turn radius, turn spacing, etc. In some studies, these parameters are optimized in a specific way to enhance the performance of a helical antenna [17]. On the other hand, in some other studies, helical antennas with modified geometry such as spherical shaped, conical shaped, and inverted conical shaped, are proposed [11, 13, 20]. A helical antenna is a natural choice for HF applications when circular polarization is desired, and, as discussed in [9, 11–13, 21], changing the geometry of standard helical antennas can help achieve wider bandwidths and other requirements while maintaining circular polarization. However, neither in these studies nor in other literature the change of a helical antenna behavior with geometrical parameters is fully investigated. In some studies, the change in only a few parameters, such as the helical antenna gain and input impedance matching, is investigated by shaping the ground conductor plane [22, 23]. There are a few studies on the design process of helical antennas. [24–27]. However, these studies do not discuss the manufacturing processes of helical antennas. Furthermore, majority of the studies in the literature investigate helical antennas for applications in the gigahertz region. To overcome the aforementioned problems and fill the gap in the literature on helical antennas in the HF band, in this study we designed a helical antenna resonating in the HF band and investigated resonance properties of the antenna with a full set of parametric simulations. The novelty of this study is that, to the best of our knowledge, it is the first study to perform a full scale parametric analysis on helical antennas designed to operate in HF band and provide a comprehensive manufacturing process. It is demonstrated that designing helical antennas with shorter length and more compact structure is possible by setting the geometrical parameters of the antennas. In addition, this study shows that it is possible to manufacture helical antennas with high stability and precision by applying the proposed exclusive and easy technique, which could also be used for the manufacturing of antennas with similar shapes.

2. Antenna design and simulations

The geometry of a helical antenna mounted on a ground plane is shown in Figure 1. In the figure, the geometrical parameters of the antenna are illustrated. Here, h and r represent the height of the antenna and turn radius measured horizontally, i.e. on an axis parallel to the ground metal plane, from the center of a turn to the center of the winding wire, respectively. Also, s and t stand for turn spacing and thickness of the winding wire,

respectively, and ρ represents the radius of the ground plane. The inset in the figure, on the other hand, is drawn to indicate the relation between the parameters in a single turn. In the inset, l and α represent the length of the wire in a single turn and pitch angle, respectively.

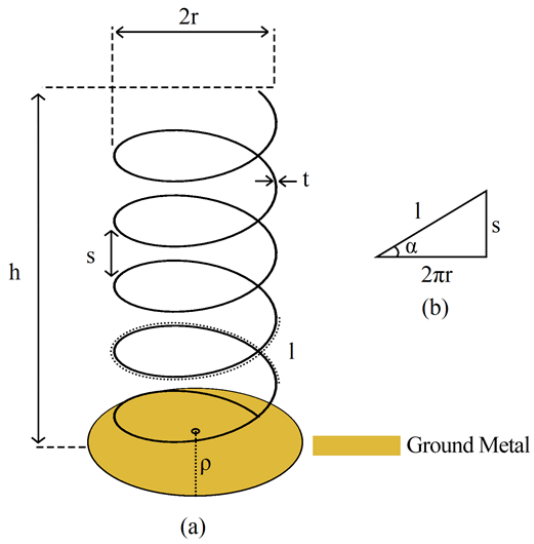

Figure 1. Helical antenna on a ground plane and its geometrical parameters. The relationship between the parameters in a single turn is also illustrated in the inset (b).

Relations between the geometrical parameters are given below, where r and s represent turn radius and spacing between the turns, as in Figure 1. Similarly, l is the wire length in a single turn and α is the pitch angle. Moreover, N and L represent the total turn number and the total length of the winding wire, respectively.

$$l = \sqrt{s^2 + (2\pi r)^2} \tag{1}$$

$$a = tan^{-1}(\frac{s}{2\pi r}) \tag{2}$$

$$L = N \times l \tag{3}$$

The designs were started with an antenna resonating in HF frequency band such that its first and second resonances occur at frequencies between 3 MHz and 30 MHz. The geometric parameters of the designed antenna are given in Table 1. As seen in the table, the height, and diameter (twice the radius) of the antenna are 31 cm and 11.65 cm, respectively. These parameters are chosen with the intention of making the antenna small in size compared to the operation wavelength, which is between 10 m (corresponding to 30 MHz frequency) and 100 m (corresponding to 3 MHz frequency). On the other hand, in the designed antenna, apart from the total wire length, the only parameter comparable with the wavelength is the radius of the ground plane, which is 1 m equal to 1/25 of a quarter of the maximum wavelength (25 m) in the HF band. The designed antenna was simulated with the help of an antenna toolbox in an electromagnetic solver. S11 parameter magnitude change of the antenna with frequency calculated in the simulations over the HF frequency band is shown in Figure 2. In the figure, it is seen that the designed antenna resonates at frequencies 11.59 MHz and 28 MHz with S11 magnitude values equal to –46.61 dB and –42.48 dB at these resonance frequencies, respectively. In addition,

the –10 dB bandwidths, i.e. frequency bandwidths at which S11 magnitude is lower than or equal to –10 dB, are found to be 0.28 MHz and 0.37 MHz, respectively. Since the higher-order resonances occur outside the HF frequency band, these resonances are not seen in the figure.

As the next step, to see their effects on antenna resonance, geometrical parameters of the antenna were changed. Firstly, the thickness of the winding wire is increased starting from 1.5 mm to 9.5 mm with a 1-mm step size while the other parameters are kept constant. The wire thickness is not considered in the literature as it is much smaller than the turn radius and other geometrical parameters; however, our study shows that the wire thickness has a considerable effect on antenna response as can be seen in Figure 3.

Table 1. Geometrical parameters of the designed antenna.

Parameter	Value
Total wire length (L)	9.89 m
Turn spacing (s)	1.00 cm
Turn radius (r)	5.825 cm
Turn number (N)	27
Ground radius (ρ)	1.00 m
Winding wire thickness (t)	1.50 mm
Height (h)	31.00 cm

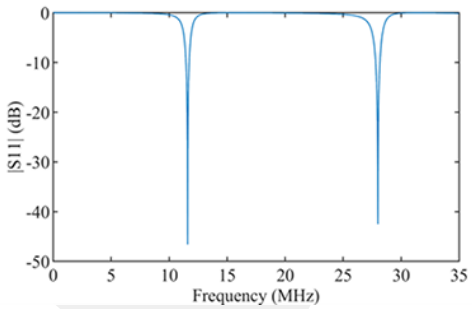

Figure 2. S11 parameter magnitude change with frequency calculated in simulations.

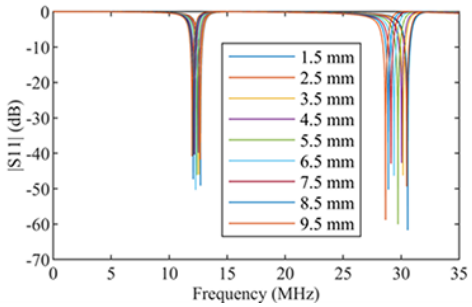

Figure 3. S11 parameter magnitude change with frequency calculated in simulations for the designed antenna having various wire thicknesses.

Figure 3 shows that both the first and second resonances shift to lower frequencies as the wire thickness increases. Also, the –10 dB bandwidth values tend to decrease as the wire thickness increases. On the other

hand, there is no regular change in S11 magnitude values at resonance frequencies resulting from the changes in wire thickness. Figure 4a and Figure 4b show the resonance and –10 dB bandwidth values for different wire thicknesses. In Figure 4a, it is observed that in the designed antenna, for all the wire thickness values, the second resonance arises at a frequency more than double of the frequency at which the first resonance occurs. Also, in Figure 4b, it can be seen that the second resonance bandwidth is wider than the first resonance bandwidth for each thickness value.

To further analyze the geometrical properties, the ground plane radius is increased from 0.07 m to 30 m with different step sizes, and simulation results are obtained. Change of S11 parameter magnitude with frequency calculated in simulations for the designed antenna having various ground plane radii is shown in Figure 5.

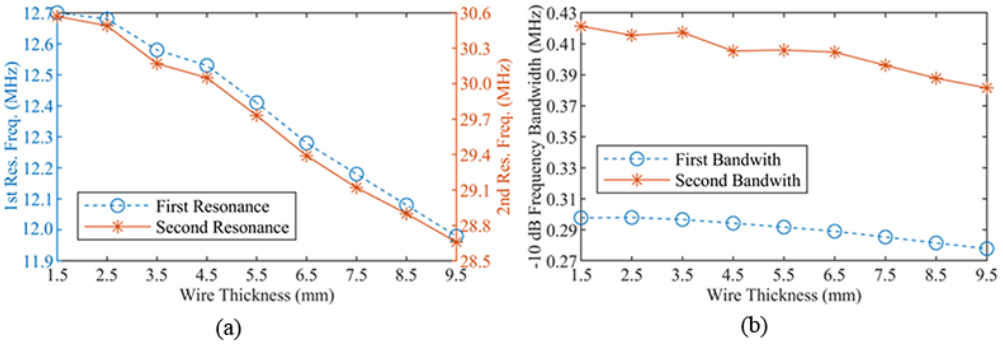

Figure 4. (a) Change of the first and second resonance frequencies with wire thickness calculated in simulations for the designed antenna. (b) Change of –10 dB bandwidth at the first and second resonance frequencies with wire thickness calculated in simulations for the designed antenna.

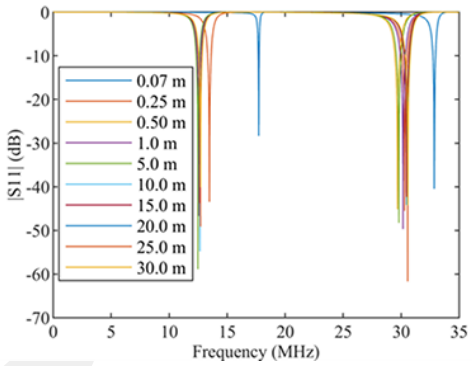

Figure 5. S11 parameter magnitude change with frequency calculated in simulations for the designed antenna having various ground plane radii.

In the figure, it is seen that both first and second resonances become more stable as the ground radius increases. For the ground radius equal to or bigger than 0.50 m, calculated resonance frequencies and –10 dB bandwidths are almost constant. In addition, the S11 parameter magnitudes calculated at the resonance frequencies are below –40 dB. It means that the designed helical antenna on a ground plane with a radius equal to or bigger than 0.50 m performs as expected. Based on this notion, the antenna prototype manufactured for testing was placed on a square-shaped ground plane with a side length equal to 1.0 m. Change of resonance frequencies and –10 dB bandwidths with ground plane radius are shown in Figures 6a and 6b, respectively.

After that, simulations were repeated to investigate the effect of the number of turns on antenna performance. In the designed antenna, the turn number is incremented from 10 to 50 with a constant step size of 5 turns, while the other parameters are kept unchanged. S11 parameter magnitude response of the antenna for different turn numbers over the entire HF band is illustrated in Figure 7.

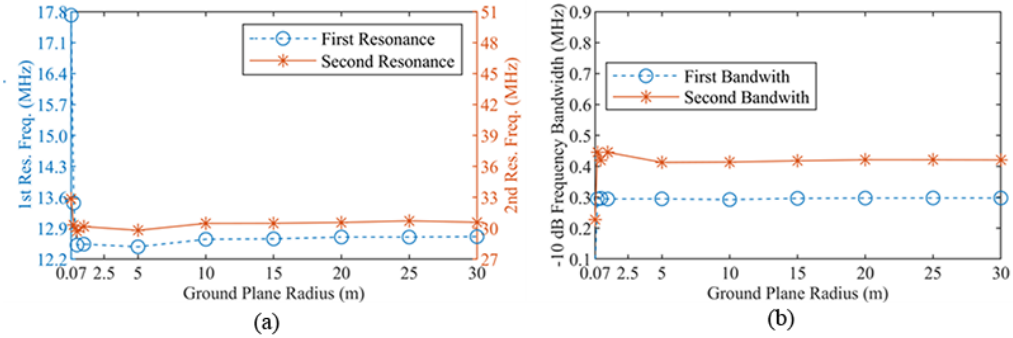

Figure 6. (a) Change of the first and second resonance frequencies with ground plane radius calculated in simulations for the designed antenna. (b) Change of –10 dB bandwidth at the first and second resonance frequencies with ground plane radius calculated in simulations for the designed antenna.

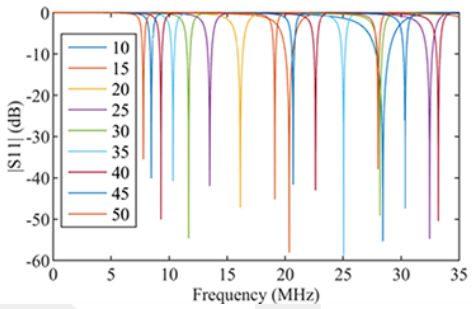

Figure 7. S11 parameter magnitude change with frequency calculated in simulations for the designed antenna having various turn numbers.

In the figure, it is observed that both first and second resonances shift to lower frequencies as the turn number increases. In addition, –10 dB bandwidths decrease with an increase in the turn number. For deeper investigation, changes in the resonance frequencies and –10 dB bandwidths with turn number are shown in Figures 8a and 8b, respectively. In the figures, second resonance frequencies for antennas with turn numbers less than 25 are not displayed. The reason for this is that when number of turns are less than 25, second resonance occurs outside the HF band, i.e. at frequencies higher than 35 MHz. Figures 4a, 6a, and 8a show that the effect of turn numbers on the antenna's resonance and bandwidth characteristics is significantly higher than the effects of wire thickness and ground plane radius. Observed shifts in resonance frequencies with turn number are explained by the fact that as the turn number increases total wire length of the antenna increases proportionally, and as the wire length increases antenna resonates at longer wavelengths and lower frequencies.

Next, simulations were repeated for the designed antenna with different spacings between wire turns. In each case, all parameters except turn spacing are the same as the parameters provided in Table 1. Spacing between turns in the antenna is increased starting from 0.25 cm to 2.75 cm with a 0.25 cm step size. Calculated S11 parameter magnitude change with frequency for different turn spacings is shown in Figure 9.

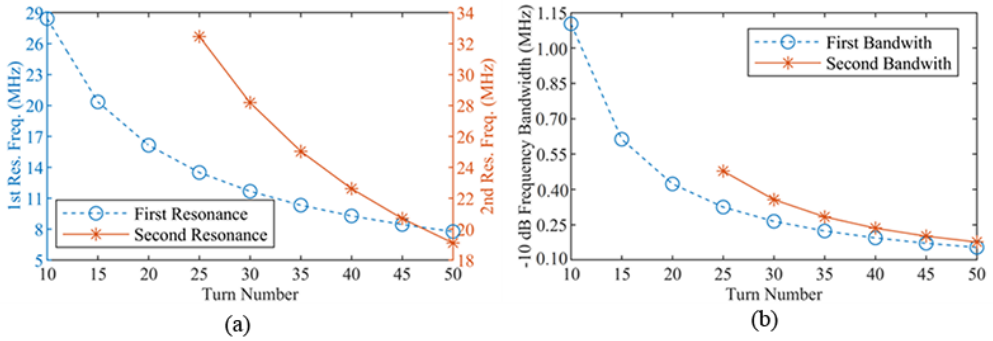

Figure 8. (a) Change of the first and second resonance frequencies with turn number calculated in simulations for the designed antenna. (b) Change of –10 dB bandwidth at the first and second resonance frequencies with turn number calculated in simulations for the designed antenna.

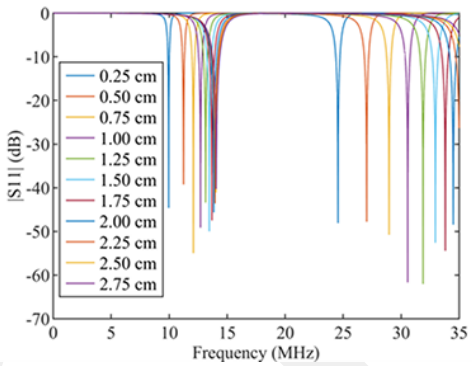

Figure 9. S11 parameter magnitude change with frequency calculated in simulations for the designed antenna having various turn spacings.

As seen, both first and second resonances shift to higher frequencies as the turn spacing increases. This is an unexpected result because as the turn spacing increases total wire length of the antenna increases proportionally. It was observed that as the turn number increases, resonances shift to lower frequencies, and this change is associated to the increased wire length of the antenna. However, although antenna wire length increases with turn spacing, resonances shift to higher frequencies. One of the possible reasons for this effect might be that if the helices of the antenna are considered as separate ring antennas stacked on top of each other as in [19], coupling between the ring antenna elements may change with their spacings. It indicates that one can shift the resonance frequencies of a helical antenna to higher and lower frequencies by increasing turn spacing and turn number, respectively, where in both cases total wire length of the antenna becomes larger. In other words, it is possible to design a helical antenna with a shorter total wire length resonating at desired frequencies by adjusting turn spacing and turn number. Manipulating these parameters result in either a decrease or an increase in the resonance frequency. In addition, in Figure 9 it is also seen that the –10 dB bandwidths widen as the turn spacing increases. On the other hand, there is no regular change in S11 magnitude values at resonance frequencies resulting from the changes in turn spacing, but it is important to note that S11 magnitude values at resonance frequencies are all below –40 dB. The changes of resonance frequencies and bandwidths in response to changes in turn spacing are seen in detail in Figures 10a and 10b, respectively. In Figure 10a, it can be seen that the rate of increase in resonance frequencies gets slower as the turn spacing increases. Furthermore, the

second resonance frequencies of the simulated antennas with turn spacings greater than 2 cm are not shown in the figures as they occur outside the HF band.

The last parameter that we investigated in our simulations is the turn radius. As in the previous analysis, simulations were obtained for the designed antenna with different turn radii. The turn radius of the designed antenna is varied from 2.5 cm to 8 cm, while the rest of the geometrical parameters are kept constant. The change of S11 parameter magnitude with frequency simulated for the designed antenna having various turn radii is shown in Figure 11.

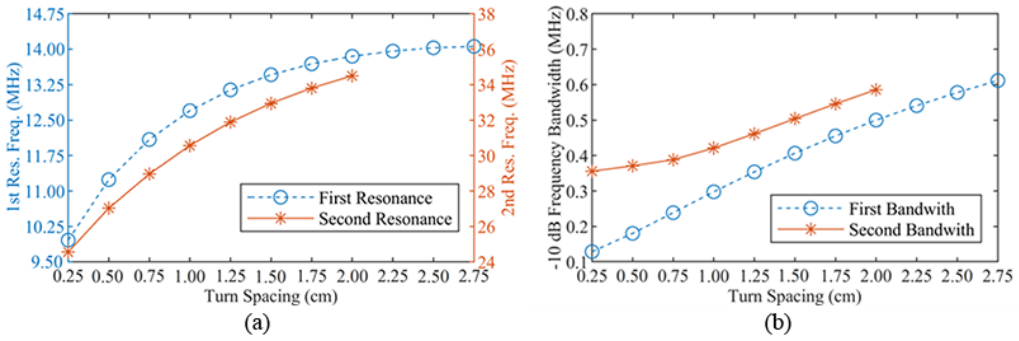

Figure 10. (a) Change of the first and second resonance frequencies with turn spacing calculated in simulations for the designed antenna. (b) Change of –10 dB bandwidth at the first and second resonance frequencies with turn spacing calculated in simulations for the designed antenna.

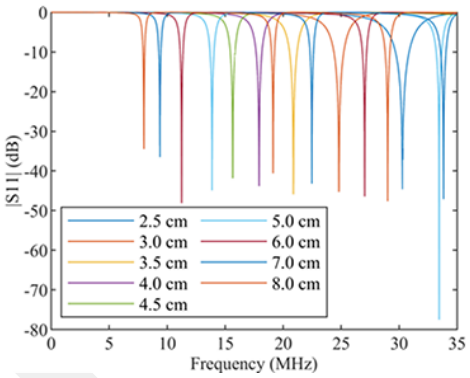

Figure 11. S11 parameter magnitude change with frequency calculated in simulations for the designed antenna having various turn radii.

In the figure, it is seen that both first and second resonances shift to lower frequencies as the turn radius of the designed antenna increases. Similar behavior was observed when we varied the turn number in the designed antenna, which can be explained by the increased wire length of the antenna. As for our analysis regarding the turn number, there is a proportional relation between the antenna's total wire length and its turn radius, and the increase in total wire length results in longer resonance wavelengths and lower resonance frequencies. As seen in the figure, compared to the effects of wire thickness, ground plane radius, and turn spacing on resonance frequencies, the effect of turn radius is more significant. In addition,–10 dB bandwidth characteristics of turn radius shows similarities to the previous analysis on turn numbers, where –10 dB bandwidth decreases as the turn radius is increased. These changes can be seen in Figures 12a and 12b, where resonance frequency and –10 dB bandwidth variations with wire turn radius are shown, respectively. Second resonance frequencies of

the antennas with turn radii less than 5 cm are not shown in these figures as these resonances occur outside the HF band. It is seen that the decreases in the resonance frequencies and bandwidths get slower as the turn radius increases.

Until this point, the parametric analysis of the designed antenna was obtained by systematically changing only one geometrical parameter each time. It is seen that increasing number of turns and turn radius of the antenna separately causes resonances to shift to lower frequencies while decreasing the bandwidths. However, it is not clear whose effect is dominant. To compare and understand the effects of turn number and turn radius, the simulations were repeated for various turn radii; however, this time turn numbers were changed simultaneously in accordance with the turn radii, such that the total antenna wire length is kept constant. S11 parameter magnitude change calculated in the simulations for the designed antenna having constant total wire length, but different turn radii and respective turn numbers are shown in Figure 13.

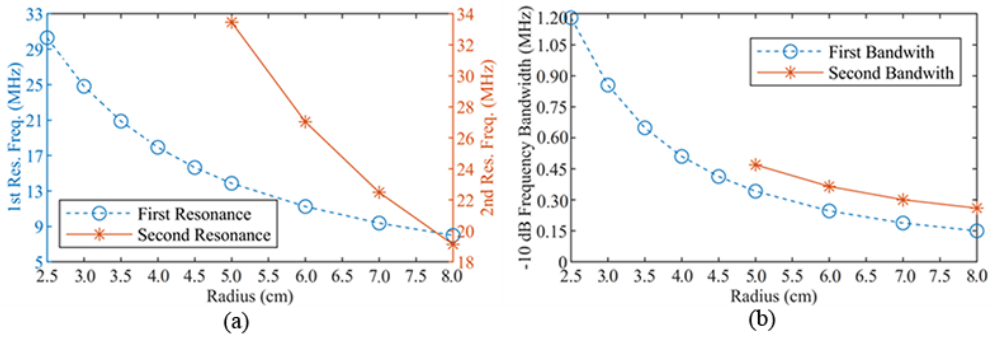

Figure 12. (a) Change of the first and second resonance frequencies with turn radius calculated in simulations for the designed antenna. (b) Change of –10 dB bandwidth at the first and second resonance frequencies with turn radius calculated in simulations for the designed antenna.

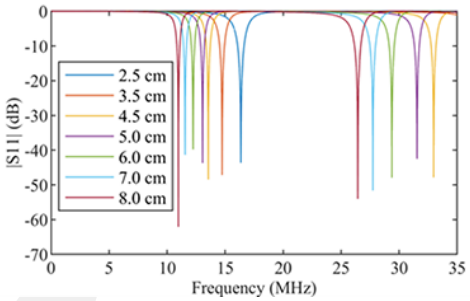

Figure 13. S11 parameter magnitude change with frequency calculated in simulations for the designed antenna having various turn numbers and turn radii such that the total wire length of the antenna is constant. Here, turn radii of 2.5 cm, 3.5 cm, 4.5 cm, 5.0 cm, 6.0 cm, 7.0 cm, and 8.0 cm correspond to turn numbers of 57.23, 41.63, 32.39, 29.16, 24.30, 20.83, and 18.23, respectively.

In the figure, it is seen that both first and second resonances shift to lower frequencies as the turn radius increases. It demonstrates that the effect of an increase in turn radius increase dominates the effect of a decrease in the turn number for resonance frequencies. However, different behaviors are observed for the bandwidths. As the turn radius increases –10 dB bandwidth around the first resonance decreases, whereas –10 dB bandwidth around the second resonance increases. These observations are clearly seen in Figures 14a and 14b, where resonance frequency and –10 dB bandwidth changes with turn radius are shown, respectively.

Radiation characteristics of the antenna with initial design parameters (see Table 1) were also calculated. Figure 15 shows the antenna's gain pattern in 3D space, and Figures 16a and 16b show the gain pattern in 2D azimuth and elevation planes, respectively, at the first resonance frequency of 11.59 MHz. As seen in the figures, omnidirectional radiation with a maximum gain of 1.7208 dBi is achieved.

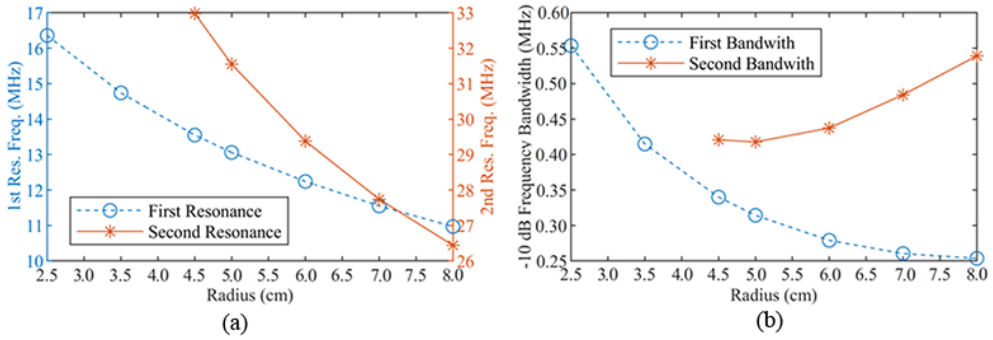

Figure 14. (a) Change of the first and second resonance frequencies with turn radius calculated in simulations for the designed antenna, where the number of turns is adjusted to set the total wire length constant. (b) Change of –10 dB bandwidth at the first and second resonance frequencies with turn radius calculated in simulations for the designed antenna, where the number of turns is adjusted to set the total wire length constant.

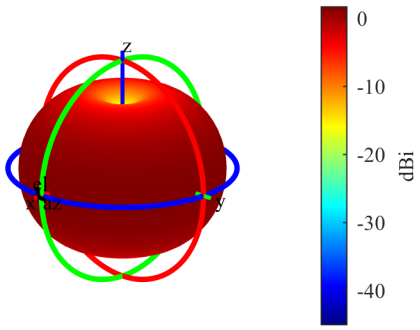

Figure 15. Gain pattern of the antenna in 3D space at its first resonance calculated in the simulations.

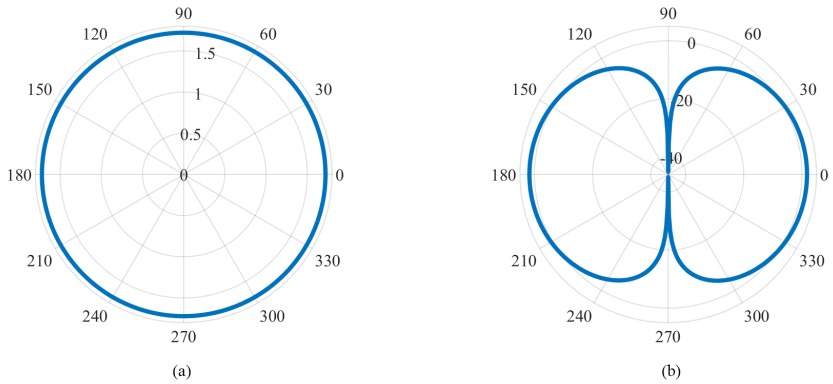

Figure 16. Gain pattern of the antenna in (a) 2D azimuth plane and (b) 2D elevation plane at its first resonance calculated in the simulations.

In addition, the impedance of the antenna was calculated. It was found to be 50–20.04j at the first resonance frequency equal to 11.59 MHz. The efficiency of the antenna was then calculated using (4). In the equation, Z_a and Z_{ref} represent the antenna impedance and reference impedance, respectively. Also, Γ and e_0 stand for the reflection coefficient and antenna efficiency. For 50 Ω reference impedance, it is found that the efficiency of the designed antenna reaches 96% at its first resonance. However, it should be noted that in the calculations material losses are ignored, i.e. the materials are assumed to be lossless.

$$\Gamma = \frac{Z_a - Z_{ref}}{Z_a + Z_{ref}}$$
$$e_0 = 1 - |\Gamma|^2 \tag{4}$$

3. Manufacturing process and measurements

After the simulations, the designed antenna was manufactured, and measurements were obtained. While manufacturing the prototype antenna, an exclusive method was followed. As the first step, to form a helix structure by winding the copper wire around it, a cylindrical shaped pipe made of PVC (polymerizing vinyl chloride) material having approximately 5.84 cm outer radius was positioned. PVC material was selected because of its very low magnetic permeability and nonconductivity. In addition, PVC is an easily accessible material with low prices, and it is rigid enough to form a basis for the windings around it. The outer radius of the PVC pipe was adjusted to be the same as the turn radius of the designed antenna that is given in Table 1. Also, the inner radius and wall thickness of the PVC pipe are 5.74 cm and 0.1 cm, respectively.

As the next step, the cylindrical geometry of the selected pipe was modeled by using three-dimensional (3D) software. After modeling the cylinder, by using the built-in functions of the software a wire with a length of 9.89 m was formed and winded around the cylinder in 27 turns with constant turn spacing of 1 cm between the turns. Then the outer surface of the cylinder was extracted as a two-dimensional (2D) planar surface. Wire turns on the cylinder surface were maintained in the form of parallel lines on the extracted 2D planar surface.

After that, the extracted 2D structures were imported to a laser cutting device and parallel lines were cut on a 1.5 mm thick cardboard material. Like PVC material, the cardboard is a nonmagnetic and nonconductive material, thus it was used in the prototype antenna. In total, 27 pieces of cardboard with rectangular geometry that represent 27 turns were manufactured. The height of these rectangles is approximately equal to the outer circumference ($2\pi \times 5.84$ cm = 36.69 cm) of the PVC pipe and their widths are equal to the turn spacing, which is 1 cm. The manufactured rectangular cardboards were then wound around and stuck outside the PVC pipe such maintaining a 1.5 mm distance from each other. This spacing between cardboard sticks is the diameter of the copper wire used in the prototype. After sticking the cardboards, as the last step, copper wire with a thickness of 1.5 mm was wrapped around the pipe to fill the empty spaces that exist between the cardboards. A photo of the manufactured antenna is shown in Figure 17. As seen in the figure, 27 wire turns exist between the cardboards. Also, the total wire length wound on the antenna is around 9.89 m and the height of the antenna, i.e. the distance between the initial and final points of the windings, is approximately 31 cm.

The manufactured antenna was then mounted on a square-shaped ground plane with a 1-m side length. The ground plane was constructed by laminating several aluminum layers one above the others. A photo of the prototype system where the manufactured antenna is mounted on the ground plane is presented in Figure 18.

Measurements were obtained with the manufactured prototype system. For comparison purposes, S11 magnitude changes with frequency over the band spanning from 0 to 35 MHz obtained in measurements and

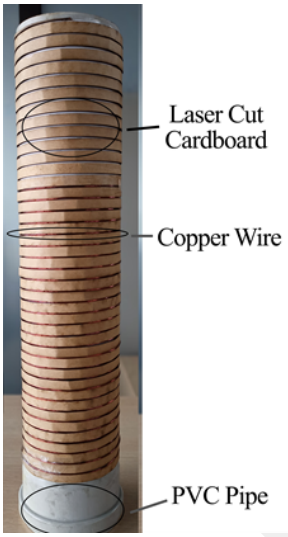

Figure 17. Prototype antenna manufactured with the proposed method and its parts.

Figure 18. The designed system with the prototype antenna placed on a square-shaped ground plane with a 1-m side length.

calculated in simulations are shown together in Figure 19. Also, in Table 2 resonance frequencies and –10 dB bandwidths around the resonances obtained in measurements and calculated in simulations are given. In the figure and the table, it is seen that the measurement results agree well with the simulation results. Small differences between the plots in the figure and the values in the table, such as very small shifts in resonance frequencies, are due to the limited precision in manufacturing and simulations, together with measurement errors. Here since sharp resonances are obtained with the designed antenna, differences between bandwidths in the table are more pronounced. Our results demonstrate the feasibility of the proposed manufacturing process, especially for the helical-shaped HF antennas.

In order to show the feasibility of the antenna and its manufacturing processes proposed in this paper, the performance comparison of the helical antenna and other HF antennas reported in the literature are given in Table 3. As seen from the table, our work enables to design and manufacture an antenna operating in the

HF band with a compact, simple and rigid structure, together with a medium gain that is comparable to the gain values of the other reported antennas.

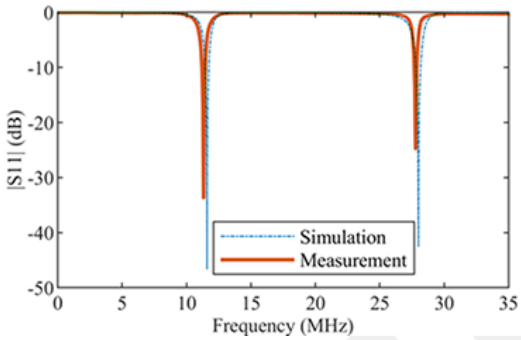

Figure 19. S11 parameter magnitude change with frequency calculated in simulations and measured in experiments for the designed prototype antenna system.

Table 2. The first and second resonance frequencies together with –10 dB bandwidths around the resonances found in measurements and calculated in simulations for the designed antenna.

Parameter	Measured	Simulated
First resonance frequency (MHz)	11.27	11.59
Second resonance frequency (MHz)	27.72	28.0
–10 dB bandwidth around the first resonance (MHz)	0.39	0.28
–10 dB bandwidth around the second resonance (MHz)	0.20	0.37

Table 3. Comparison of our work with other HF antennas given in the literature.

Antenna type	Polarization	Mounting standards	Rigid structure	Dimensions	Operating frequency	Gain
[28] Helical array	Linear	Simple	No	1 m × 1.2 m	3–30 MHz	Not specified
[29] Helical	Linear	Simple	No	2 m × 0.1 m	3–30 MHz	Not specified
[30] Log-periodic	Not specified	Complex	Yes	> 5 m × 5 m	14–40 MHz	9 dB
[31] Two-arm inverted L	Linear	Complex	No	8 m × 3.8 m × 1 m	3–10 MHz	> –20 dBi
[32] Log-periodic	Linear	Not specified	Not specified	8.682 m × 8.178 m	18–20 MHz	Not specified
[33] Bifolded-monopole	Not specified	Complex	No	12 m × 2 m	2–50 MHz	> 2 dB
Our work	Linear	Simple	Yes	0.31 m × 0.1165 m	3–30 MHz	1.7208 dBi

4. Conclusion

In this study, a helical antenna operating in HF frequency band is designed, and with a full set of simulations resonance behavior change of the antenna is investigated. Due to its 3D structure, the designed antenna has

sizes much smaller than the operation wavelength such that except for the total wire length, the only geometrical parameter that is comparable with the wavelength is the ground plane radius. In the simulations, first, only a single parameter was altered in each case and changes of resonance frequencies and –10 dB bandwidths at the resonance frequencies were calculated. Results show that as the winding wire thickness increases the first and second resonances of the designed antenna that arise in the HF band shift to lower frequencies. Also, –10 dB bandwidths calculated at the resonance frequencies decrease as opposed to the increase in the wire thickness. Although wire thickness is not taken into account in other literature, because it is much smaller in size compared to other parameters of the helical antenna, obtained results demonstrate that it is one of the key parameters that significantly affect the antenna resonance. On the other hand, in the simulations, it is observed that as the ground radius increases, antenna resonances become more stable such that for the designed antenna with a ground radius equal to or bigger than 0.50 m, the resonance frequencies and –10 dB bandwidths at these resonances are calculated to be almost constant. This is an expected result, and it is the reason why a square-shaped ground plane with a 1-m side length is mounted to the back of the prototype manufactured antenna.

Moreover, simulation results show that first and second resonances shift to lower frequencies as the number of turns or turn radius increases, which was also observed before in the winding wire thickness analysis. It is explained by the increased length of the winding wire. As the turn number or turn radius increases, the total length of the winding wire increases proportionally, and it results in longer resonance wavelengths and lower resonance frequencies. Also, similar to winding wire results, it is seen that –10 dB frequency bandwidths at resonances decrease with the increases in turn number and turn radius. However, further simulations obtained with controlling the antennas turn spacing parameter exhibit different results. It is found that both the first and second resonances shift to higher frequencies and –10 dB bandwidths at the resonances widen as the turn spacing enhances, which is unexpected. Unlike the number of turns and turn radius simulations, here resonance frequencies shift to higher frequencies as the turn spacing increases, although total wire length increases with the turn spacing. This is a key result, and it indicates that one can design a helical antenna with shorter wire length and compact sizes resonating at desired frequencies by adjusting its geometrical parameters.

The effects of the parameters turn number and turn radius found to have more significant impact on the antenna's resonance and bandwidth characteristics. In additional simulations, for the designed antenna with constant total wire length, it is observed that the resonances shift to lower frequencies as the turn radius increases in spite of the decrease in turn number. However, as the turn radius increases despite the decrease in turn number –10 dB bandwidth around the first resonance decreases while –10 dB bandwidth around the second resonance increases. It shows that on resonance frequency shifts and –10 dB bandwidth around the first resonance the effect of turn radius increase in the designed antenna dominates the effect of the decrease in turn number, but it is not valid for the –10 dB bandwidth around the second resonance.

To verify simulation results, the designed antenna was fabricated with an exclusive manufacturing process and measurements were obtained. While manufacturing, first the pipe and the wire windings were modeled in 3D, and then the outer surface of the pipe and the wire turns on it were extracted on a 2D planar surface. The extracted 2D structures were imported to a laser-cutting device and parallel lines corresponding to wire turns were cut on a cardboard material. The produced rectangular shape cardboards were wound and stuck around the pipe with a constant spacing equal to wire thickness. As the last step, the wire was wrapped and stuck around the pipe to fill the empty spaces between the cardboard. The manufactured helical antenna was mounted on a ground plane containing many thin aluminum sheets laminated on top of each other. Thanks to the followed process, a helical antenna with a rigid structure was manufactured with high accuracy. As

expected, measurement results obtained with the manufactured antenna agree well with the simulation results. With a complete set of analyses, this study fills the gap that exists in the literature for resonance behavior change of helical antennas. Also, the study demonstrates the feasibility of helical antenna designs with shorter wire length and compact sizes resonating at desired frequencies. With the proposed manufacturing process, it is possible for the first time in literature to prototype rigid helical antennas in high accuracy with low cost. We believe that the proposed manufacturing process is promising for the production of other wire antenna types having 3D architecture.

References

[1] Headrick JM, Thomason JF. Applications of high-frequency radar. Radio Science 1998; 33: 1045-1054.

[2] Moore E. Performance Evaluation of HF Aircraft Antenna Systems. IRE Transactions on Antennas and Propagation 1958; 6 (3): 254-260.

[3] Tan ZY, Mansor MF. Monopole Antenna for Communication System of Military Vehicle at HF Band 3-30 MHz. In: 2021 IEEE Globecom 15th Malaysia International Conference on Communication (MICC), 2021, pp. 102-107.

[4] Freeman RL, Freeman RL. High-Frequency (HF) Radio Systems. In: Reference Manual for Telecommunications Engineering, 2002.

[5] International Telecommunication Union, Radio Communication Sector of ITU (ITU-R). Recommendation ITU-R M.1798-2: Characteristics of HF radio equipment for the exchange of digital data and electronic mail in the maritime mobile service, 2021.

[6] Dhar S, Perry BD. Equalized Megahertz-Bandwidth HF Channels for Spread Spectrum Communications. MILCOM 1982- IEEE Military Communications Conference- Progress in Spread Spectrum Communications 1982: 29:5-1-29.5-5

[7] Underhill MJ. Comparison of the predicted performance of typical HF and VHF Yagi-Uda antennas with the theoretical limit of all their elements being driven 2000; 163-168.

[8] Bod M, Ahmadi-Boroujeni M, Mohammadpour-Aghdam K. Broadband loaded monopole antenna with a novel on-body matching network. AEU - International Journal of Electronics and Communications 2016; 70: 1551-1555.

[9] D Hawkins J, Lok LB, V Brennan P, Nicholls KW. HF Wire-Mesh Dipole Antennas for Broadband Ice-Penetrating Radar. IEEE Antennas and Wireless Propagation Letters 2020; 19: 2172-2176.

[10] Erhel Y, Perrine C, Chatellier C, Bourdon P, Lemur D. High data rate radio communications through the ionospheric channel. AEU - International Journal of Electronics and Communications 2007; 61: 270-278.

[11] Kenkel M, Wong T. Parametric analysis of the transverse bilateral helical antenna. In 2008 IEEE Antennas and Propagation Society International Symposium 2008: 1-4.

[12] Abdullah S, Syed Hassan SI. Design small size of High Frequency (HF) helical antenna. In 2009 5th International Colloquium on Signal Processing & Its Applications 2009: 259-262.

[13] Abdullah S, Md Sharif J, Ishak NH, Zanal A, Amat Mushim MA et al. Simulation for High Frequency (HF) range of helical antenna. In 2010 International Conference on Science and Social Research (CSSR 2010) 2010: 396-400.

[14] Balanis CA. Antenna Theory: Analysis and Design. John Wiley & Sons, 2015.

[15] Cardoso J, Safaai-Jazi A. A spherical helical antenna. In Proceedings of IEEE Antennas and Propagation Society International Symposium, 1993, pp. 1558-1561.

[16] Jimisha K, Kumar S. Optimum Design of Exponentially Varying Helical Antenna with Non Uniform Pitch Profile. Procedia Technology 2012; 6: 792-798.

[17] Kraus JD. Helical Beam Antennas for Wide-Band Applications. Proceedings of the IRE 1948; 36: 1236-1242.

[18] Safaai-Jazi A, Cardoso JC. Radiation characteristics of a spherical helical antenna. IEE Proceedings - Microwaves, Antennas and Propagation 1996; 143: 7-12.

[19] Volakis JL. Antenna Engineering Handbook, Fourth Edition. McGraw-Hill Education, 2007.

[20] Fartookzadeh M, Mohseni Armaki SH. Multi-band conical and inverted conical printed quadrifilar helical antennas with compact feed networks. AEU - International Journal of Electronics and Communications 2016; 70: 33-39.

[21] SINGH RP, SINGH RN. Helical antenna for satellite transmission†. International Journal of Electronics 1973; 34: 601-607.

[22] Djordjevic AR, Zajic AG, Ilic MM. Enhancing the gain of helical antennas by shaping the ground conductor. IEEE Antennas and Wireless Propagation Letters 2006; 5: 138-140.

[23] Wadkar SP, Hogade BG, Rathod SM, Kumar H, Kumar G. Normal Mode Helical Antenna on Small Circular Ground Plane. IETE Journal of Research 2020; 66: 617-624.

[24] Fusco VF. Foundations of antenna theory and techniques. Harlow Munich: Pearson Prentice-Hall, 2005.

[25] Salbani MF, Abdul Halim MA, Jahidin AH, Megat Ali MSA. Helical antenna design for wireless power transmission: A preliminary study. In 2011 IEEE International Conference on System Engineering and Technology, 2011, pp. 192-195.

[26] Wong J, King H. Empirical helix antenna design. In 1982 Antennas and Propagation Society International Symposium, 1982, pp. 366-369.

[27] Kedze KE, Wang H, Park I. Effects of Split Position on the Performance of a Compact Broadband Printed Dipole Antenna with Split-Ring Resonators. Journal of Electromagnetic Engineering and Science, 2019; 19: 115-121.

[28] Baker J, Iskander MF, Youn HS, Celik N. High-performance compact HF antenna for radar and communication applications. In 2010 IEEE Antennas and Propagation Society International Symposium, 2010:1-4.

[29] Gulati G, Abdelrahman AH, Tang , Xin H. Passive and Active Matching of Electrically-Small Helical Antenna for HF-Band Communications. In 2017 IEEE International Symposium on Antennas and Propagation, USNC/URSI 2017: 733-734.

[30] Ram K. HF Voice Data Communication Between DEAL, Dehradun and Maitri, Antarctica. Eleventh Indian Expedition to Antarctica, Scientific Report. Department of Ocean Development, Technical Publication, 1995; 9: 337-340.

[31] Sanghai SA, Ignatenko M, Filipovic DS. Low-Profile Two-Arm Inverted-L Antenna Design for Vehicular HF Communications. In IEEE Transactions on Antennas and Propagation, 2017; 65 (11): 5710-5719.

[32] Boswell A. Antennas for a 19 MHz groundwave radar. In: 1995 Ninth International Conference on Antennas and Propagation, ICAP'95 1995; 1: 463-464.

[33] Mattioni L, Marocco G. Design of a broadband HF antenna for multimode naval communications. In IEEE Antennas and Wireless Propagation Letters, 2005, 4: 179-182.